Event-Based Contrastive Learning for Medical Time Series

Nassim Oufattole[1*]　　　　　　　　　　　　　　　　　NASSIM@MIT.EDU

Hyewon Jeong[1*]　　　　　　　　　　　　　　　　　HYEWONJ@MIT.EDU

Matthew Mcdermott[2]　　　　　MATTHEW_MCDERMOTT@HMS.HARVARD.EDU

Aparna Balagopalan[1]　　　　　　　　　　　　　　　APARNAB@MIT.EDU

Bryan Jangeesingh[1]　　　　　　　　　　　　　　　BRYTECH@MIT.EDU

Marzyeh Ghassemi[1]　　　　　　　　　　　　　　MGHASSEM@MIT.EDU

Collin Stultz[1,2]　　　　　　　　　　　　　　　　CMSTULTZ@MIT.EDU

[1] *Massachusetts Institute of Technology, Cambridge, MA, USA*

[2] *Harvard Medical School, Boston, MA, USA*

arXiv:2312.10308v4 [cs.LG] 8 Aug 2024

Abstract

In clinical practice, one often needs to identify whether a patient is at high risk of adverse outcomes after some key medical event. For example, quantifying the risk of adverse outcomes after an acute cardiovascular event helps healthcare providers identify those patients at the highest risk of poor outcomes; i.e., patients who benefit from invasive therapies that can lower their risk. Assessing the risk of adverse outcomes, however, is challenging due to the complexity, variability, and heterogeneity of longitudinal medical data, especially for individuals suffering from chronic diseases like heart failure. In this paper, we introduce Event-Based Contrastive Learning (EBCL) - a method for learning embeddings of heterogeneous patient data that preserves temporal information before and after key index events. We demonstrate that EBCL can be used to construct models that yield improved performance on important downstream tasks relative to other pretraining methods. We develop and test the method using a cohort of heart failure patients obtained from a large hospital network and the publicly available MIMIC-IV dataset consisting of patients in an intensive care unit at a large tertiary care center. On both cohorts, EBCL pretraining yields models that are performant with respect to a number of downstream tasks, including mortality, hospital readmission, and length of stay. In addition, unsupervised EBCL embeddings effectively cluster heart failure patients into subgroups with distinct outcomes, thereby providing information that helps identify new heart failure phenotypes. The contrastive framework around the index event can be adapted to a wide array of time-series datasets and provides information that can be used to guide personalized care.

1. Introduction

Healthcare providers often aspire to identify a patient's risk of a future adverse event after some index event, such as an inpatient admission or intubation in the ICU. Prediction of such risks is important for the development of effective treatment strategies (Rahimi

---
* Equal contribution.

et al., 2014) and for ensuring that healthcare resources are allocated appropriately (Duong et al., 2021; Jencks et al., 2009). This has motivated researchers to study a variety of learning algorithms, including directly supervised (Zhang et al., 2021; Rajkomar et al., 2018), self-supervised (Tipirneni and Reddy, 2022; Labach et al., 2023; Jeong et al., 2023) and contrastive learning algorithms (Hyvarinen and Morioka, 2017; Agrawal et al., 2022) for identifying patients at the highest risk of adverse outcomes.

Many contrastive learning methods (and more generally, representation learning methods) for medical time series data (Agrawal et al., 2022; Tipirneni and Reddy, 2022; Labach et al., 2023) strive to create latent representations that preserve temporal trends within the data. These approaches, however, generally ignore the fact that some portions of medical time series data are more informative than others. For example, data surrounding key medical events (e.g., an admission for a heart attack, or an admission associated with a new cancer diagnosis) are rich in information that plays a significant role in patient prognostication.

Our approach, Event-Based Contrastive Learning (EBCL), diverges from existing work (Hyvarinen and Morioka, 2017; Agrawal et al., 2022; Dave et al., 2022) by imposing a specialized pretraining contrastive loss solely on data around critical events, where the most clinically-relevant information regarding disease progression and prognosis is likely to be found. EBCL is a contrastive learning method, meaning it defines a latent space structure leveraging positive and negative pairs—where positive pairs of points should be close and negative pairs far apart in the latent space. In particular, we use patient data immediately before and after a key medical event as positive pairs, and data from different patients as negative pairs (Figure 1). The resulting embedding maps data surrounding key medical events to similar regions of the latent space, thereby encoding temporal trends.

We evaluate EBCL on two datasets: a private, multi-site cohort of heart failure patients and a cohort of intensive care unit (ICU) patients derived from MIMIC-IV (Johnson et al., 2023). Experiments are performed under a traditional pretraining/finetuning regime, in which model parameters are first initialized with EBCL pretraining and then specialized by task-specific finetuning. We perform empirical comparisons with published pretraining systems for the medical domain. *We present finetuning results showing that EBCL consistently outperforms these baselines across all tasks and all events.* Furthermore, beyond traditional fine-tuning, we also show that EBCL embeddings produce informative representations of patient states. *Linear probing with frozen EBCL embeddings on the heart failure cohort achieves AUCs at least* 4.38 *points higher than other methods for predicting Mortality and* 12.99 *points higher for predicting Length of Stay.* EBCL embeddings further yield highly expressive clusters that heart failure patients into distinct phenotypes, forming a basis for disease subtyping. With ablation studies, we demonstrate that the advantages of EBCL are uniquely due to its focus on temporal trends immediately surrounding key medical events. Finally, we reproduce these improvements on downstream tasks using mechanical ventilation and hypotension events in the ICU setting. Overall, our results strongly demonstrate the benefits of domain-specific latent space structure learning through its focus on key medical events and its unique temporal contrastive loss formulation. In summary, our contributions are as follows:

- We propose a new contrastive pretraining method for time series data that encodes patient-specific temporal trends around key medical events in clinical data.

- We demonstrate that this formalism leads to improved predictive performance on downstream outcome prediction tasks, outperforming published pretraining baselines and supervised models.

- EBCL pretraining alone generates embeddings that are useful for identifying high-risk subgroups based on patient-specific temporal trends. This suggests these contrastive pretraining methods may be useful beyond downstream task prediction and for patient subtyping.

Generalizable Insights about Machine Learning in the Context of Healthcare

Our results demonstrate that accounting for the clinical importance of key medical events explicitly during representation learning can significantly improve the quality of representations learned and eventual downstream performance, offering significant advantages over a variety of published baselines on several finetuning tasks over two clinical datasets. This simultaneously (1) underscores the utility of incorporating clinical domain knowledge into machine learning in healthcare, (2) demonstrates a beautifully simple approach to inject this domain knowledge during learning in a way that is both performant and efficient, and (3) produces models that can further better integrate with the realities of event-focused clinical workflows where key medical alerts or decision support tasks are often triggered by specific events in the clinical setting (e.g., prediction of readmission after discharge or of patient decompensation after negative cardiovascular events in intensive care). We believe that not only can the success of our explicit pre-training strategy, EBCL, generalize to other medical datasets and tasks, but also that this mechanism of incorporating domain knowledge by better contrasting temporal dynamics before and after key areas of clinical change may be helpful for both future research into health AI and for the generation of models that can be more closely integrated into event-centric clinical decision support settings in practice.

2. Related Works

Representation Learning for Clinical Time-Series Data   Medical time series datasets pose unique challenges due to their inherently high-dimensional and irregularly sampled nature, and the significant presence of missing data (Shukla and Marlin, 2020). These complexities demand focused strategies to encode (Tipirneni and Reddy, 2022) and represent such time-series data (Li and Marlin, 2020; Tipirneni and Reddy, 2022; Lee et al., 2023; McDermott et al., 2023a; Labach et al., 2023) to enhance model performance, particularly in scenarios with limited data. Decision tree baselines, such as XGBoost (Chen and Guestrin, 2016) remain competitive for both tabular and tabular time series data (Labach et al., 2023; Shwartz-Ziv and Armon, 2022). Many pretraining methods have also been explored, which include forecasting (STraTS) (Tipirneni and Reddy, 2022) masked imputation (DuETT) (McDermott et al., 2021; Labach et al., 2023), and weakly supervised methods (McDermott et al., 2021). More recently, contrastive learning methods (Agrawal et al., 2022; Hyvarinen and Morioka, 2017; King et al., 2023) have been applied to time series and multimodal temporal data, which is known to impose deeper structural constraints on latent space geometry (McDermott et al., 2023b) motivating them as a better option for the pretraining

objectives. We focus on advancing contrastive learning methods for time series data to impose and leverage meaningful latent space structures for downstream tasks.

Contrastive Learning for Medical Time-Series Data Contrastive learning is a form of self-supervised learning (SSL) that uses positive and negative pairs of instances (Franceschi et al., 2019; Tonekaboni et al., 2021; Eldele et al., 2021; Hyvarinen and Morioka, 2017; Agrawal et al., 2022; Oord et al., 2018; Kiyasseh et al., 2021; Raghu et al., 2023; Jeong et al., 2023). Such techniques may use (1) automatically co-occurring sources of information (Liang et al., 2022; Raghu et al., 2023; Zhang et al., 2022; Heiliger et al., 2022), (2) augmented versions of the same information (Eldele et al., 2021; Oord et al., 2018; Radford et al., 2021; Kiyasseh et al., 2021; Li et al., 2022; Raghu et al., 2023; Oh et al., 2022; Gopal et al., 2021; Cheng et al., 2020), (3) similar data instances with smaller distances to one another (Jeong et al., 2023), or (4) temporal proximity (Franceschi et al., 2019; Tonekaboni et al., 2021) to generate positive and negative pairs. Compared to previous works defining views based on temporal proximity (Franceschi et al., 2019; Tonekaboni et al., 2021), EBCL defines views based both on domain-informed index events and temporal proximity around them.

3. Event-Based Contrastive Learning (EBCL) for Medical Time-Series

3.1. Problem Formulation

We use a formalism introduced in past work (Tipirneni and Reddy, 2022) to model heterogeneous time series data: Let $\mathcal{D}$ be a dataset containing N patient trajectories, $\{X_1, \cdots, X_N\}$. A patient trajectory $X_i = [x_{i,1}, x_{i,2}, \ldots, x_{i,M_i}]$ is a chronologically ordered sequence of patient i's $M_i \in \mathbb{N}$ observations. Each observation $x_{i,j}$ corresponds to an individual medical event (e.g., a laboratory test) and is encoded as a triple $x_{i,j} = (t_{i,j}, o_{i,j}, v_{i,j})$ where $t_{i,j}$ is the time of the observation, $o_{i,j}$ denotes what medical result is being measured (e.g., what lab test is being observed), and $v_{i,j}$ is the actual value of the observation. For example, if a patient has a potassium test (encoded via $o = 7$) taken at time $t = $ "12/1/2022, 11:30 a.m." which reports a value of 4.2 mEq/L, then their corresponding patient trajectory would contain a triple $(t_{i,j}, o_{i,j}, v_{i,j}) = ($"2/1/2024, 8:00 a.m.", $7, 4.2)$.

To define the patient windows that EBCL will contrast during pre-training, we define the following. Given a window size $\tau \in \mathbb{N}$, let $t_{i,j}$ be the timestamp of a clinical index event (e.g., a hospital admission) and define $L_i^j \subset X_i$ to be a subset of patient i's trajectory consisting of the τ events prior to $t_{i,j}$ and $R_i^j \subset X_i$ be the subsequent τ events including and after $t_{i,j}$:

$$L_i^j = [x_{i,j-\tau}, x_{i,j-\tau+1}, \ldots, x_{i,j-1}]$$
$$R_i^j = [x_{i,j}, x_{i,j+1}, \ldots, x_{i,j+\tau-1}].$$

3.2. Model Optimization Pipeline

We consider a two-stage learning problem where we pretrain a network f_θ and fine-tune on the outcome prediction tasks that are of interest.
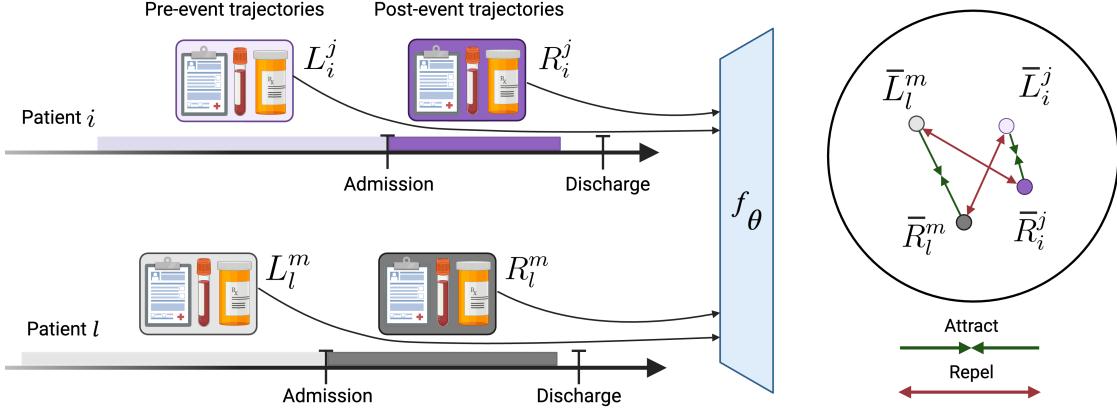
Figure 1: **Event-based contrastive learning (EBCL).** For patient i and event j, we denote pre-event data, L_i^j, and post-event data, R_i^j. For EBCL pretraining, we sample a batch, $\mathcal{B}$, of pre and post-event trajectory pairs from a dataset, $D_{\mathcal{B}} = \{(L_i^j, R_i^j) : i, j \in \mathcal{B}\}$. We choose the event of interest to be an inpatient admission. L_i^j and R_i^j are passed separately into a transformer encoder f_θ to get $\bar{L}_i^j = f_\theta(L_i^j)$ and $\bar{R}_i^j = f_\theta(R_i^j)$ which is pretrained with CLIP contrastive loss. The positive pairs are pre and post-event data of the same event, $(\bar{L}_i^j, \bar{R}_i^j)$. The negative pairs are mismatched pre-event and post-event trajectories from different patients, such as $(\bar{L}_i^j, \bar{R}_l^m)$ where $i \neq l$.

EBCL Pretraining For pretraining a model, we sample an event and its corresponding pre-event and post-event dataset. We use a model, f_θ as an encoder, and get pre- and post-embeddings $f_\theta(L_i^j)$ and $f_\theta(R_i^j)$. We then compute the CLIP loss $\mathcal{L}_{\text{CLIP}}$ (Radford et al., 2021) on a batch of these embeddings, where (L_i^j, R_l^m) is a positive pair if $i = l$ and $j = m$. Intuitively, CLIP loss pushes together representations of positive pairs (i.e. paired left and right windows) and repels representations of negative pairs (i.e. mismatched left and right windows) as depicted in Figure 1.

Finetuning During fine-tuning, we use encoder f_θ to get representations finetuned for downstream outcome classification tasks. We use negative cross-entropy loss, $\mathcal{L}_{\text{CE}}$. For tasks involving both pre- and post-event data (such as predicting 1-year mortality following hospital discharge, where 'pre' refers to data prior to admission and 'post' refers to data during admission but prior to discharge), we obtain embeddings of both $(f_\theta(L_i^j)$ and $f_\theta(R_i^j))$ and pass them through a shallow feedforward network (see Appendix Figure 8) to arrive at a prediction for our label, y_i^j. For tasks that only use data prior to the key medical event (such as predicting if hospital length of stay will be greater than 1 week given only pre-admission event data), we pass only the pre-data embedding $(f_\theta(L_i^j))$ to the shallow feedforward network. EBCL weights after pretraining are used to initialize this model for the downstream tasks defined in Section 4.1. Furthermore, to prevent dataset leakage, we ensured the label y_i^j of heart failure cohort (1-Year Mortality, 30-Day Readmission) to

happen at least one day after the end of R_i^j. For predicting the length of stay (LOS) of the heart failure cohort and for predicting In-ICU Mortality and LOS of the MIMIC-IV cohort, we only use the pre-representation $f_\theta(L_i^j)$, and to avoid data leakage, outcomes must be at least one day after the end of L_i^j.

4. Dataset and Methods

In this section, we introduce the dataset, outcome prediction tasks, and baseline models we used for the experiment.[1]

4.1. Dataset and Tasks

We demonstrated our method using two datasets: a private dataset containing multi-site medical records of a heart failure cohort and the public MIMIC-IV ICU medical record dataset.

4.1.1. Heart Failure Dataset

Dataset We have assembled a multi-site cohort of $107,268$ patients with a prior diagnosis of heart failure. This cohort includes patient within a single hospital system with multiple locations (i.e. one hospital and its satellite locations). Collectively, this cohort had $383,254$ inpatient admissions, obtained from the electronic data warehouse of a large hospital network. The dataset includes patient trajectories over a maximum span of 40 years and a maximum number of $3,275$ features, which includes labs, diagnoses, procedures, medications, tabular echocardiogram recordings, physical measurements (weight, height), and admissions/discharges. In our heart failure cohort described in Table 1, we restrict our clinical events to inpatient admissions that have at least 16 data points for both pre-admission and post-admission data. If a patient has no such event, they were not included in the cohort. We partitioned our compiled dataset into training (80%), validation (10%), and testing (10%) with the split stratified so that no patients overlapped across splits. Additional information on dataset preprocessing is provided in the appendix Section B.

Table 1: **Statistics for finetuning datasets from the electronic health record of Heart Failure cohort.**

	Heart Failure Cohort (Event: Inpatient Admission)		
Task	# Patients	# Events	# Prevalence
Readmission	65,435	262,734	26.8%
Mortality	52,748	195,747	30.6%
LOS	107,268	383,254	54.1%

---

1. Code used for the experiment is available at: https://github.com/mit-ccrg/ebcl

Tasks We finetune and evaluate on three binary downstream tasks: 30-day readmission, 1-year mortality, and 7-day LOS. The task of predicting 30-day readmission has been chosen for the heart failure cohort due to its critical importance for hospitals. This metric is financially significant, as hospitals face penalties under the Centers for Medicare & Medicaid Services Readmission Reduction Program, which cost them over half a billion dollars in 2017 (Upadhyay et al., 2019). The datasets are summarized in Table 1. Note that for the LOS task, we only use Pre-Admission data as input, as Post-Admission data would leak the LOS outcome. We also always restrict Post-Admission data, R_n^i, to the data prior to patient discharge, as this is the information that will be available at decision time for the 1-year mortality and 30-day readmission tasks.

4.1.2. MIMIC IV (JOHNSON ET AL., 2023)

Dataset and Events MIMIC IV (Johnson et al., 2023) is a public EHR dataset with ICU stay of patients admitted to Beth Israel Deaconess Medical Center between 2008 and 2019. We have assembled a cohort of patients who have hospital stay records and experienced the key events that frequently happen within the ICU (Table 2). We utilize two medical events:

- **Hypotension:** any time point where mean arterial pressure (invasive MAP or non-invasive NIMAP) transitions from over 60 to below 60 mmHg.

- **Mechanical Ventilation:** the start of a mechanical ventilation procedure.

Table 2: **Statistics for finetuning datasets from the electronic health record of MIMIC-IV ICU cohort.**

Task	# Event-Type	# Patients	# Stays	# Events	# Prevalence
		MIMIC-IV ICU Cohort			
Mortality	Hypotension	35,234	47,567	342,884	17.1%
LOS	Hypotension	35,234	47,567	342,884	48.1%
Mortality	Mechanical Ventilation	23,269	26,955	31,420	13.4%
LOS	Mechanical Ventilation	23,269	26,955	31,420	52.7%

Tasks We finetune models on two binary outcome prediction tasks related to acute patient status in the ICU: In-ICU mortality and 3-day LOS, motivated by previous works (Alghatani et al., 2021; Nguyen et al., 2021; Zhang and Kuo, 2024; McDermott et al., 2021; Wang et al., 2020). As post-event (hypotension, mechanical ventilation) could leak the outcome label as it could include the time horizon until the outcome, we limit the dataset to the dataset prior to the event for fine-tuning.

4.2. Model Architecture

For all experiments, unless specified otherwise, we use a transformer encoder as the backbone of our architecture (Figure 8). The encoder has two encoder layers with the input of 512

observation sequences followed by a 128-dimension feed-forward layer between self-attention layers, and 32-dimension token embeddings. We then perform Fusion Self-Attention (Tipirneni and Reddy, 2022; Raffel and Ellis, 2015), by taking an attention-weighted average of the output embeddings of the transformer to get a single 32-dimension embedding. Finally, we have a linear projection to a 32-dimension embedding. Input sequences are required to have a length of at least 16 observations and are padded to a length of 512. Attention over padded tokens is masked in the transformer and the Fusion Self-Attention layer. This is the exact architecture from the paper (Tipirneni and Reddy, 2022) except we use a 128 dimension feed-forward layer instead of 2048 as this improved the supervised baselines in initial experiments.

4.3. Baseline methods

To evaluate our method, we perform experiments with the following baselines and dataset preparation methods. For more information on methods, see Appendix Section B.

XGBoost (Chen and Guestrin, 2016): XGBoost is a tree boosting-based machine learning algorithm, widely used for classification and regression tasks with tabular datasets, and a competitive baseline for time-series prediction tasks (McDermott et al., 2023a).

Supervised Transformer (S-Trans) : This corresponds to standard supervised training without EBCL pretraining. The transformer model f_θ is initialized with random weights, and then the model is trained in a supervised fashion for a specific task.

Order Contrastive Pretraining (OCP) (Agrawal et al., 2022): We take a continuous sequence of at most 512 tokens, split the sequence in half, and randomly swap the first and second halves (Appendix Figure 5). We pretrain f_θ with the OCP objective for each patient i where the pretraining task is to discriminate correct and switched sequencing.

Self-supervised Transformer for Time-Series (STraTS) (Tipirneni and Reddy, 2022): STraTS represents transformer-based forecasting of time-series data. The transformer-based architecture they proposed is designed for handling sparse and irregularly sampled multivariate clinical time-series data.

Dual Event Time Transformer (DuETT) (Labach et al., 2023): DuETT proposes a masked imputation pretraining task for detecting the presence of a feature and its value.

4.4. Finetuning and Downstream Outcome Prediction

We finetune the pretrained models (OCP, STraTS, DuETT, and EBCL) with a single fully connected layer to predict outcomes. We perform an extensive learning rate and dropout hyperparameter search for pretraining and finetuning and use a maximum of 300 epochs for pretraining and 100 epochs for finetuning. More details are provided in the Appendix Section B.3. We take the epoch with the highest validation set performance for pretraining and finetuning. We pretrain our models and run 5 random seeds for finetuning and report the mean and standard deviation of results across these seeds.

5. Experiments and Results

We present the following key results: 1) EBCL outperforms all baselines on fine-tuning tasks. 2) EBCL yields richer embeddings than competitor pretraining models, as assessed on the heart failure cohort. 3) The definition of the domain-informed event and its closeness to the sampled event are key to our performance gains.

5.1. EBCL Outperforms All Baselines in the Heart Failure Dataset

In addition to EBCL, we consider several baseline methods for comparison. XGBoost builds a representation that summarizes information along the long period of clinical time series. OCP (Agrawal et al., 2022) learns features that are sensitive to temporal reversal (which are called *least time reversible features*). STraTS (Tipirneni and Reddy, 2022) is designed to learn features that are useful for forecast observations during inpatient stays, which helps build a representation that captures relevant features and temporal dependencies. DuETT (Labach et al., 2023) representation learns missingness-invariant representations of data from masked imputation for accurate downstream prediction robust to missingness of input pretraining data. Each time-series pretraining baseline model learns distinct features that, in principle, help the model perform better for subsequent finetuning clinical outcome classification tasks. By contrast, EBCL learns patient-specific temporal trends associated with specific index medical events.

Table 3: **EBCL Pretraining improves results over a supervised baseline and time-series pretraining baselines in the Heart Failure Dataset.** For the heart failure cohort, we summarize the downstream finetuning performance using both the area under the receiver operating characteristic (AUC) of three prediction tasks (30-Day Readmission, 1-Year Mortality, and 1-Week Length of Stay (LOS)) averaged over 5 runs with different seeds. We present finetuning performance on the MIMIC-IV Dataset for the outcomes of in-ICU Mortality and 3-Day LOS. Across all tasks, EBCL results (boldfaced) were statistically significantly better than all other tested models.

	Heart Failure Cohort		
	30-Day Readmission	1-Year Mortality	1-Week LOS
XGBoost	70.85 ± 0.08	80.33 ± 0.19	79.74 ± 0.10
S-Trans	70.28 ± 0.16	81.54 ± 0.24	88.74 ± 0.48
OCP	70.27 ± 0.32	80.06 ± 0.29	90.06 ± 0.25
STraTS	70.06 ± 0.11	79.95 ± 0.62	88.36 ± 1.09
DueTT	69.51 ± 0.50	79.39 ± 0.16	75.35 ± 0.61
EBCL	$\mathbf{71.66 \pm 0.03}$	$\mathbf{82.43 \pm 0.07}$	$\mathbf{90.98 \pm 0.05}$

EBCL achieves a significant improvement over all baseline models for three predictive tasks (1-Year Mortality, 30-Day Readmission, 1-Week LOS) in the heart failure dataset

(Table 3, 10). We note that pretraining methods can often achieve improved performance relative to a supervised baseline when the pretraining dataset is significantly larger than the finetuning datasets (Devlin et al., 2019; Dosovitskiy et al., 2020). However, in this case, EBCL achieves better performance over the supervised baseline even though the pretraining and finetuning datasets are of similar size. Consequently, the improvement in performance arises from solving the contrastive learning task and not the fact that pretraining leverages a larger dataset. Contrasting around our index event better captures temporal trends than other contrastive and generative pretraining methods.

5.2. EBCL Embeddings are More Informative than Other Baselines

Linear Probing To gauge the extent to which the pretrained embeddings contain important information that can be leveraged for downstream predictive tasks, we employed a linear probing evaluation on the heart failure cohort. This involved fitting a logistic regression classifier on the frozen embeddings generated by the model. The coefficient for L2 regularization was tuned. We compute the mean and standard deviation of logistic regression results over 5 seeds of pretraining each method, and results are reported in Table 4 and 11.

Table 4: **Linear Probing for Evaluating the Pretrained Embeddings.** EBCL (boldfaced) yielded the embedding that performs the best across all tasks.

	30-Day Readmission	1-Year Mortality	1-Week LOS
OCP	65.04 ± 0.39	70.34 ± 0.83	58.75 ± 0.23
STraTS	60.88 ± 0.75	65.33 ± 0.99	57.37 ± 0.96
DuETT	58.39 ± 3.61	63.52 ± 6.71	55.29 ± 1.61
EBCL	$\mathbf{65.40 \pm 0.16}$	$\mathbf{74.72 \pm 0.36}$	$\mathbf{71.74 \pm 2.08}$

Frozen EBCL representations consistently outperformed other baseline methods for all three tasks evaluated (Table 4, 11). We additionally see dramatic improvements when using a KNN classifier (results and methodology are in Appendix Section C). This implies that neighbors within the EBCL latent space are more similar in outcomes than those derived from any other baseline model, which indicates that EBCL inherently realizes a latent space that naturally stratifies outcomes.

Heart Failure Outcome Subtyping with EBCL Representations We further explore the extent to which the learned embedding space naturally stratifies patient outcomes of interest, and find that EBCL embeddings are highly indicative of patient outcomes. In particular, using K-means clustering with $K = 6$ (determined using elbow method as described in Appendix F.1), we see that EBCL clusters correspond to distinct heart failure patient subgroups. We compare the distributions of time-to-next-readmission and time-to-mortality (Figure 11 (b) and (c)), and using a t-test with p-value threshold 0.01, we find a significant difference between the time-to-outcome distributions of patients in any two clus-
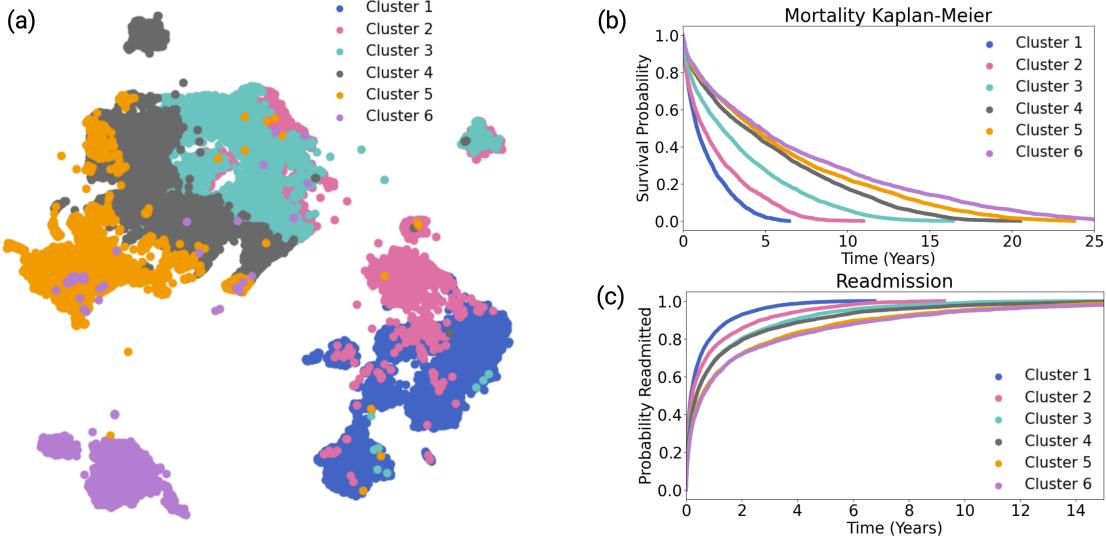
Figure 2: **Clustering and outcome risk subtyping from pretrained EBCL Embedding. (a)** Clustering and dimensionality reduction of pretrained embedding showed distinct heart failure clusters with unique outcome prognoses. Clusters are sorted by the prevalence of 1-Year Mortality (cluster 1 is the fatal group with the highest mortality rate, while cluster 6 is the healthiest group). The survival curve of the identified clusters plotting **(b)** time to mortality and **(c)** time to readmission

ters. These relationships also hold on the outcome prevalence of each cluster. The cluster 1 had the highest risk of 1-year mortality (53.9%) and 30-day readmission (34.1%) rate; in contrast, patients in cluster 6 had a more favorable prognosis with a lower risk of 1-year mortality (21.0%) and 30-day readmission (18.8%).

5.3. EBCL Generalizes to Acute Patient Cohort of MIMIC-IV ICU

The applications above (Table 3, 4) focus on applications of EBCL in a large heart failure cohort derived from several tertiary care centers, where the index event was hospital admission (Figure 1). To determine whether the approach is fruitful in other cohorts, and with other types of index events, we applied EBCL to the MIMIC-IV cohort (Johnson et al., 2023), which consists of patients admitted to an ICU at a major tertiary care center. We explored two key medical events: 1) hypotensive episodes (defined as a mean arterial pressure < 60mmHg) and 2) mechanical ventilation. The outcomes of interest included In-ICU mortality and 3-day length of ICU stay. Across all tasks and events, EBCL yields the highest AUC for both finetuning (Table 5, 12) and linear probing (Table 6, 13) for predicting outcomes, compared with the baselines.

Table 5: **EBCL Pretraining improves downstream outcome prediction over a supervised baseline and time-series pretraining baselines in the MIMIC-IV cohort.** We summarize the finetuning performance using two metrics: area under the receiver operating characteristic (AUC) of two prediction tasks (In-ICU Mortality and 3-Days Length of Stay (LOS)). The result has averaged over 5 runs with different seeds.

	MIMIC-IV Hypotension		MIMIC-IV Mechanical Ventilation	
	In-ICU Mortality	3-Day LOS	In-ICU Mortality	3-Day LOS
XGBoost	80.07 ± 0.12	80.19 ± 0.20	81.45 ± 0.05	77.96 ± 0.05
S-Trans	81.92 ± 0.32	80.46 ± 0.14	83.65 ± 10.31	80.55 ± 0.10
OCP	81.89 ± 0.21	80.34 ± 0.09	88.99 ± 0.18	80.51 ± 0.13
STraTS	82.73 ± 0.20	80.46 ± 0.06	88.99 ± 0.18	80.51 ± 0.13
DueTT	64.94 ± 1.75	73.33 ± 2.47	52.00 ± 0.71	48.28 ± 10.04
EBCL	$\mathbf{83.02 \pm 0.08}$	$\mathbf{80.70 \pm 0.03}$	89.20 ± 0.35	81.36 ± 0.05

Table 6: **Linear Probing for Evaluating the Pretrained Embeddings.** EBCL (boldfaced) yielded the embedding that performs the best across all tasks.

	MIMIC-IV Hypotension		MIMIC-IV Mechanical Ventilation	
	In-ICU Mortality	3-Day LOS	In-ICU Mortality	3-Day LOS
OCP	69.86 ± 0.67	72.13 ± 0.36	68.99 ± 1.92	68.25 ± 0.41
STraTS	72.13 ± 1.36	73.06 ± 1.11	73.76 ± 0.64	69.58 ± 0.39
DueTT	72.37 ± 1.29	74.94 ± 0.71	51.29 ± 0.00	58.16 ± 0.01
EBCL	$\mathbf{77.80 \pm 0.44}$	$\mathbf{77.95 \pm 0.43}$	$\mathbf{79.26 \pm 1.27}$	$\mathbf{75.85 \pm 0.63}$

5.4. Ablation Studies

Performance Gains Observed with EBCL were Uniquely due to Key Event and Closeness of Data The novelty of our method arises from 1) leveraging the clinically important event and 2) using the data around the index event. We perform a series of ablation studies on the heart failure cohort to analyze the effect of defining the event and sampling observations around the event.

Effect of the definition of event We evaluate the importance of selecting a clinically significant event for pretraining by selecting non-inpatient admission events. We first use any non-inpatient visits as the EBCL index event (such as outpatient visits or emergency unit visits) instead of inpatient admission (**Non-Adm EBCL**). Our standard EBCL model,

which uses inpatient hospital admission as the index event, outperformed an approach that specifically excludes inpatient admissions from the event set (Table 7).

As the Non-Adm EBCL experiments include encounters with the emergency room, we also performed a second set of experiments where events were restricted to only outpatient encounters (thereby excluding all emergency department encounters). These **Outpatient EBCL** experiments also underperformed standard EBCL. These results highlight the critical role of inpatient admissions in learning consistent patterns for predicting clinically significant outcomes, suggesting that the context around inpatient events is essential for optimal model performance in this cohort.

Table 7: **Ablation Studies**. We compare the EBCL variants by applying various definitions of events and different sampling strategies. We summarize the downstream finetuning performance (AUROC) of three prediction tasks averaged over 5 runs with different seeds, where we boldface statistically significant results. *Note that FT stands for finetuning data and the entry both means both pre and post data are used, but for predicting 1-Week LOS we always only used the Pre-event dataset to avoid data leakage.

	Index Event	FT*	30-Day Readmission	1-Year Mortality	1-Week LOS
EBCL	Inpatient	Both	**71.66 ± 0.03**	**82.43 ± 0.07**	**90.98 ± 0.05**
Censoring	Inpatient	Both	70.63 ± 0.10	81.35 ± 0.04	90.43 ± 0.11
Non-Adm	Non-Inpatient	Both	70.73 ± 0.11	81.89 ± 0.10	90.12 ± 0.17
Outpatient	Outpatient	Both	70.51 ± 0.14	81.80 ± 0.03	89.68 ± 0.14
Pre Event	Inpatient	Pre	70.48 ± 0.09	79.63 ± 0.06	✗
Post Event	Inpatient	Post	69.20 ± 0.09	80.36 ± 0.03	✗

Effect of Censoring Observations We evaluate the importance of sampling observations locally around the index event by introducing a censoring window around the EBCL inpatient admission index event (**EBCL with Censoring**). In this experiment, we sample consecutive input observation points that are away from the index event by setting the censoring window (Appendix Figure 10). Pre-event observations were chosen from the window preceding the censoring window before the index event. Post-event observations were chosen from the window following the censoring window after the index event. EBCL with Censoring demonstrated lower performance compared to the standard EBCL (Table 7). This outcome reinforces the fundamental advantage of EBCL, which capitalizes on the proximity of data around the index event. Hence, leveraging data close to the index event is crucial for the model's effectiveness in clinical prediction tasks.

6. Discussion

6.1. EBCL pretraining improves Outcome Stratification in Temporally Rich Problem Setting

Our experimental results on both heart failure and MIMIC-IV ICU patient records show the generalizability of our method on different clinical time-series datasets. This experiment was meaningful in demonstrating the effectiveness of defining medically critical tasks for specific cohorts and leveraging time-series datasets surrounding them that are useful for downstream risk stratification of critically ill patient cohorts. Notably, EBCL showed superiority over other methods in capturing patient status, which is emphasized by improved clustering. These results underscore the robustness of EBCL in handling complex clinical time-series data.

6.2. Event Centricity Aligned with Clinical Workflow Contributes to Improved Risk Stratification

Our method is most appropriate in settings where we have temporal sequences of datasets and some knowledge about what types of events are likely to be clinically most meaningful. We demonstrated our method using event-centric downstream outcome prediction tasks for acute and chronic patient care scenarios. The primary use case, exemplified in this paper, is to predict cardiovascular outcomes specifically for the heart failure cohort using the in-hospital time-series dataset. Heart failure provides a particularly good application domain because the trajectory of patients with heart failure is punctuated by frequent hospital admissions, where each admission is associated with a further decrease in myocardial function (Gheorghiade et al., 2005); i.e., hospital admissions are particularly important in the health trajectory of these patients. For this application, we relied on prior domain knowledge about heart failure in general and its pathophysiology to identify what types of clinical events are likely to be most impactful.

For the domain-informed events of the ICU dataset, we used the two most prevalent events corresponding to ICU stay: hypotension and mechanical ventilation. However, depending on the cohort of interest and the downstream task of interest the key event could include other medically important events like acidosis, alkalosis, sepsis, and hypoxia.

The identification of relevant 'events' to guide EBCL pretraining need not be restricted to hospital admissions. An event, for example, can encompass different clinical occurrences, including episodes of hypoglycemia in diabetic patients, a new diagnosis of hypertension made at an outpatient visit, etc. The key insight is that a key medical event is one where important clinical features change and/or new trends in the patient's clinical trajectory are expected. EBCL provides event-centric learning of health data which reflects the real-world clinical workflows. By doing so, EBCL not only captures the essential dynamics of patient care but also significantly improves risk stratification, providing a robust foundation for critical healthcare decisions.

6.3. Limitations and Future Work

There are several limitations and areas for future work that EBCL inspires. Firstly, the effective application of the EBCL requires preliminary domain knowledge to identify suitable

events for pretraining. This limits the applicability of EBCL in settings in which domain knowledge is not available, or in which finetuning tasks are not related to the events chosen for use during pre-training. Adapting EBCL to work in settings both where domain knowledge is either unavailable or partially available and in areas where finetuning tasks require more flexibility in how they relate to the key medical events used in pre-training are two areas of future work that could thus extend EBCL's generalizability to different clinical settings. Another area of future work could be to extend EBCL's contrastive loss framework to incorporate additional notions of similarity between patients or portions of patient records in addition to colocation around key medical events, such as future patient diagnoses or adverse events. This could enrich the geometry in the learned representation space by EBCL and capture deeper, more clinically meaningful relationships. Finally, the EBCL pretraining objective can be extended to additional modalities of health data with or multimodal health datasets.

7. Conclusion

EBCL, a novel pretraining scheme for medical time series data, learns patient-specific temporal representations around clinically significant events. We demonstrate that the method outperforms previous contrastive, generative, and supervised baselines on 3 different finetuning tasks over two clinical datasets. We further show that EBCL pretraining generates a rich latent space characterized by: 1) significant improvements in classification performance with linear probing on EBCL latent space and 2) improvement in identifying high risk patient subgroups using embeddings arising from EBCL pretraining alone. From a set of ablation studies, we show that the key to performance gains in EBCL is from the introduction of the event and the nearness of data around that index event. These results demonstrate key insights about representation learning over medical record data that underscore the importance of integrating domain knowledge and provide a translatable vehicle to do so, which will improve and extend the state of research in health AI overall.

References

Monica N Agrawal, Hunter Lang, Michael Offin, Lior Gazit, and David Sontag. Leveraging time irreversibility with order-contrastive pre-training. In *International Conference on Artificial Intelligence and Statistics*, pages 2330–2353. PMLR, 2022.

Khalid Alghatani, Nariman Ammar, Abdelmounaam Rezgui, and Arash Shaban-Nejad. Predicting intensive care unit length of stay and mortality using patient vital signs: Machine learning model development and validation. *JMIR Medical Informatics*, 9(5): e21347, May 2021. ISSN 2291-9694. doi: 10.2196/21347. URL http://dx.doi.org/10.2196/21347.

Tianqi Chen and Carlos Guestrin. Xgboost: A scalable tree boosting system. In *Proceedings of the 22nd acm sigkdd international conference on knowledge discovery and data mining*, pages 785–794, 2016.

Joseph Y Cheng, Hanlin Goh, Kaan Dogrusoz, Oncel Tuzel, and Erdrin Azemi. Subject-aware contrastive learning for biosignals. *arXiv preprint arXiv:2007.04871*, 2020.

Ishan Dave, Rohit Gupta, Mamshad Nayeem Rizve, and Mubarak Shah. TCLR: Temporal contrastive learning for video representation. *Computer Vision and Image Understanding*, 219:103406, jun 2022. doi: 10.1016/j.cviu.2022.103406. URL https://doi.org/10.1016%2Fj.cviu.2022.103406.

Jacob Devlin, Ming-Wei Chang, Kenton Lee, and Kristina Toutanova. Bert: Pre-training of deep bidirectional transformers for language understanding, 2019.

Alexey Dosovitskiy, Lucas Beyer, Alexander Kolesnikov, Dirk Weissenborn, Xiaohua Zhai, Thomas Unterthiner, Mostafa Dehghani, Matthias Minderer, Georg Heigold, Sylvain Gelly, et al. An image is worth 16x16 words: Transformers for image recognition at scale. In *International Conference on Learning Representations*, 2020.

William N Dudley, Rita Wickham, and Nicholas Coombs. An introduction to survival statistics: Kaplan-Meier analysis. *Journal of the advanced practitioner in oncology*, 7(1): 91, 2016.

Son Q Duong, Le Zheng, Minjie Xia, Bo Jin, Modi Liu, Zhen Li, Shiying Hao, Shaun T Alfreds, Karl G Sylvester, Eric Widen, et al. Identification of patients at risk of new onset heart failure: Utilizing a large statewide health information exchange to train and validate a risk prediction model. *Plos one*, 16(12):e0260885, 2021.

Emadeldeen Eldele, Mohamed Ragab, Zhenghua Chen, Min Wu, Chee Keong Kwoh, Xiaoli Li, and Cuntai Guan. Time-series representation learning via temporal and contextual contrasting. *arXiv preprint arXiv:2106.14112*, 2021.

Jean-Yves Franceschi, Aymeric Dieuleveut, and Martin Jaggi. Unsupervised scalable representation learning for multivariate time series. *Advances in neural information processing systems*, 32, 2019.

Mihai Gheorghiade, Leonardo De Luca, Gregg C. Fonarow, Gerasimos Filippatos, Marco Metra, and Gary S. Francis. Pathophysiologic targets in the early phase of acute heart failure syndromes. *The American Journal of Cardiology*, 96(6):11–17, September 2005. ISSN 0002-9149. doi: 10.1016/j.amjcard.2005.07.016. URL http://dx.doi.org/10.1016/j.amjcard.2005.07.016.

Bryan Gopal, Ryan Han, Gautham Raghupathi, Andrew Ng, Geoff Tison, and Pranav Rajpurkar. 3kg: Contrastive learning of 12-lead electrocardiograms using physiologically-inspired augmentations. In *Machine Learning for Health*, pages 156–167. PMLR, 2021.

Lars Heiliger, Anjany Sekuboyina, Bjoern Menze, Jan Egger, and Jens Kleesiek. Beyond medical imaging-a review of multimodal deep learning in radiology. *TechRxiv*, (19103432), 2022.

Aapo Hyvarinen and Hiroshi Morioka. Nonlinear ICA of Temporally Dependent Stationary Sources. In Aarti Singh and Jerry Zhu, editors, *Proceedings of the 20th International Conference on Artificial Intelligence and Statistics*, volume 54 of *Proceedings of Machine Learning Research*, pages 460–469. PMLR, 20–22 Apr 2017. URL https://proceedings.mlr.press/v54/hyvarinen17a.html.

Stephen F Jencks, Mark V Williams, and Eric A Coleman. Rehospitalizations among patients in the medicare fee-for-service program. *New England Journal of Medicine*, 360 (14):1418–1428, 2009.

Hyewon Jeong, Collin M Stultz, and Marzyeh Ghassemi. Deep metric learning for the hemodynamics inference with electrocardiogram signals. In *Machine Learning for Healthcare Conference*, pages 321–342. PMLR, 2023.

Alistair EW Johnson, Lucas Bulgarelli, Lu Shen, Alvin Gayles, Ayad Shammout, Steven Horng, Tom J Pollard, Sicheng Hao, Benjamin Moody, Brian Gow, et al. MIMIC-IV, a freely accessible electronic health record dataset. *Scientific data*, 10(1):1, 2023.

Ryan King, Tianbao Yang, and Bobak J. Mortazavi. Multimodal pretraining of medical time series and notes. In Stefan Hegselmann, Antonio Parziale, Divya Shanmugam, Shengpu Tang, Mercy Nyamewaa Asiedu, Serina Chang, Tom Hartvigsen, and Harvineet Singh, editors, *Proceedings of the 3rd Machine Learning for Health Symposium*, volume 225 of *Proceedings of Machine Learning Research*, pages 244–255. PMLR, 10 Dec 2023. URL https://proceedings.mlr.press/v225/king23a.html.

Dani Kiyasseh, Tingting Zhu, and David A Clifton. Clocs: Contrastive learning of cardiac signals across space, time, and patients. In *International Conference on Machine Learning*, pages 5606–5615. PMLR, 2021.

Alex Labach, Aslesha Pokhrel, Xiao Shi Huang, Saba Zuberi, Seung Eun Yi, Maksims Volkovs, Tomi Poutanen, and Rahul G Krishnan. DuETT: Dual event time transformer for electronic health records. In *Machine Learning for Healthcare Conference*, pages 403–422. PMLR, 2023.

Kwanhyung Lee, Soojeong Lee, Sangchul Hahn, Heejung Hyun, Edward Choi, Byungeun Ahn, and Joohyung Lee. Learning missing modal electronic health records with unified multi-modal data embedding and modality-aware attention. In *Machine Learning for Healthcare Conference*, pages 423–442. PMLR, 2023.

Liam Li, Kevin Jamieson, Afshin Rostamizadeh, Ekaterina Gonina, Jonathan Ben-Tzur, Moritz Hardt, Benjamin Recht, and Ameet Talwalkar. A system for massively parallel hyperparameter tuning. *Proceedings of Machine Learning and Systems*, 2:230–246, 2020.

Steven Cheng-Xian Li and Benjamin Marlin. Learning from irregularly-sampled time series: A missing data perspective. In *International Conference on Machine Learning*, pages 5937–5946. PMLR, 2020.

Yikuan Li, Mohammad Mamouei, Gholamreza Salimi-Khorshidi, Shishir Rao, Abdelaali Hassaine, Dexter Canoy, Thomas Lukasiewicz, and Kazem Rahimi. Hi-BEHRT: Hierarchical Transformer-based model for accurate prediction of clinical events using multimodal longitudinal electronic health records. *IEEE journal of biomedical and health informatics*, 27(2):1106–1117, 2022.

Victor Weixin Liang, Yuhui Zhang, Yongchan Kwon, Serena Yeung, and James Y Zou. Mind the gap: Understanding the modality gap in multi-modal contrastive representation learning. *Advances in Neural Information Processing Systems*, 35:17612–17625, 2022.

Matthew B. A. McDermott, Bret Nestor, Evan Kim, Wancong Zhang, Anna Goldenberg, Peter Szolovits, and Marzyeh Ghassemi. A comprehensive EHR timeseries pre-training benchmark. In *Proceedings of the Conference on Health, Inference, and Learning*, pages 257–278, 2021.

Matthew B. A. McDermott, Bret Nestor, Peniel N Argaw, and Isaac S. Kohane. Event stream GPT: A data pre-processing and modeling library for generative, pre-trained transformers over continuous-time sequences of complex events. In *Thirty-seventh Conference on Neural Information Processing Systems Datasets and Benchmarks Track*, 2023a. URL https://openreview.net/forum?id=hiO0735tmc.

Matthew B. A. McDermott, Brendan Yap, Peter Szolovits, and Marinka Zitnik. Structure-inducing pre-training. *Nature Machine Intelligence*, pages 1–10, 2023b.

Leland McInnes, John Healy, Nathaniel Saul, and Lukas Großberger. UMAP: Uniform Manifold Approximation and Projection. *Journal of Open Source Software*, 3(29), 2018.

A Tuan Nguyen, Hyewon Jeong, Eunho Yang, and Sung Ju Hwang. Clinical risk prediction with temporal probabilistic asymmetric multi-task learning. In *Proceedings of the AAAI Conference on Artificial Intelligence*, volume 35, pages 9081–9091, 2021.

Jungwoo Oh, Hyunseung Chung, Joon-myoung Kwon, Dong-gyun Hong, and Edward Choi. Lead-agnostic self-supervised learning for local and global representations of electrocardiogram. In *Conference on Health, Inference, and Learning*, pages 338–353. PMLR, 2022.

Aaron van den Oord, Yazhe Li, and Oriol Vinyals. Representation learning with contrastive predictive coding. *arXiv preprint arXiv:1807.03748*, 2018.

Alec Radford, Jong Wook Kim, Chris Hallacy, Aditya Ramesh, Gabriel Goh, Sandhini Agarwal, Girish Sastry, Amanda Askell, Pamela Mishkin, Jack Clark, et al. Learning transferable visual models from natural language supervision. In *International conference on machine learning*, pages 8748–8763. PMLR, 2021.

Colin Raffel and Daniel PW Ellis. Feed-forward networks with attention can solve some long-term memory problems. *arXiv preprint arXiv:1512.08756*, 2015.

Aniruddh Raghu, Payal Chandak, Ridwan Alam, John Guttag, and Collin Stultz. Sequential multi-dimensional self-supervised learning for clinical time series. In *International Conference on Machine Learning*, pages 28531–28548. PMLR, 2023.

Kazem Rahimi, Derrick Bennett, Nathalie Conrad, Timothy M Williams, Joyee Basu, Jeremy Dwight, Mark Woodward, Anushka Patel, John McMurray, and Stephen MacMahon. Risk prediction in patients with heart failure: a systematic review and analysis. *JACC: Heart Failure*, 2(5):440–446, 2014.

Alvin Rajkomar, Eyal Oren, Kai Chen, Andrew M Dai, Nissan Hajaj, Michaela Hardt, Peter J Liu, Xiaobing Liu, Jake Marcus, Mimi Sun, et al. Scalable and accurate deep learning with electronic health records. *NPJ digital medicine*, 1(1):18, 2018.

Ville Satopaa, Jeannie Albrecht, David Irwin, and Barath Raghavan. Finding a "kneedle" in a haystack: Detecting knee points in system behavior. In *2011 31st International Conference on Distributed Computing Systems Workshops*, pages 166–171, 2011. doi: 10.1109/ICDCSW.2011.20.

Satya Narayan Shukla and Benjamin M Marlin. A survey on principles, models and methods for learning from irregularly sampled time series. *arXiv preprint arXiv:2012.00168*, 2020.

Ravid Shwartz-Ziv and Amitai Armon. Tabular data: Deep learning is not all you need. *Information Fusion*, 81:84–90, 2022.

Sindhu Tipirneni and Chandan K Reddy. Self-supervised transformer for sparse and irregularly sampled multivariate clinical time-series. *ACM Transactions on Knowledge Discovery from Data (TKDD)*, 16(6):1–17, 2022.

Sana Tonekaboni, Danny Eytan, and Anna Goldenberg. Unsupervised representation learning for time series with temporal neighborhood coding. *arXiv preprint arXiv:2106.00750*, 2021.

Soumya Upadhyay, Amber L Stephenson, and Dean G Smith. Readmission rates and their impact on hospital financial performance: a study of washington hospitals. *INQUIRY: The Journal of Health Care Organization, Provision, and Financing*, 56: 0046958019860386, 2019.

Shirly Wang, Matthew BA McDermott, Geeticka Chauhan, Marzyeh Ghassemi, Michael C Hughes, and Tristan Naumann. Mimic-extract: A data extraction, preprocessing, and representation pipeline for mimic-iii. In *Proceedings of the ACM conference on health, inference, and learning*, pages 222–235, 2020.

Min Zhang and Tsung-Ting Kuo. Early prediction of long hospital stay for intensive care units readmission patients using medication information. *Computers in Biology and Medicine*, 174:108451, May 2024. ISSN 0010-4825. doi: 10.1016/j.compbiomed.2024. 108451. URL http://dx.doi.org/10.1016/j.compbiomed.2024.108451.

Xiang Zhang, Marko Zeman, Theodoros Tsiligkaridis, and Marinka Zitnik. Graph-guided network for irregularly sampled multivariate time series. In *International Conference on Learning Representations*, 2021.

Yuhao Zhang, Hang Jiang, Yasuhide Miura, Christopher D Manning, and Curtis P Langlotz. Contrastive learning of medical visual representations from paired images and text. In *Machine Learning for Healthcare Conference*, pages 2–25. PMLR, 2022.

Appendix A. Views of Contrastive Learning

In this section, we outline the contrastive learning framework of EBCL and its variations compared to the contrastive baseline (OCP (Agrawal et al., 2022)) and specify some examples of what information they learn throughout pretraining. Our proposed method (EBCL) takes positive and negative samples (A, B) or (C, D) from the same patient's medical record, where window A or C immediately precedes window B or D in time in the original medical record (Algorithm 1). Furthermore, windows A and C immediately precede a key medical event (e.g., inpatient admission), and windows B and D immediately follow that same key medical event in the original medical record. EBCL uses negative sample pairs (A, D) or (C, B) from different patients' medical records, where, for instance, A immediately precedes a key medical event and D immediately follows a key medical event in the original medical record. Our EBCL variants (EBCL Censored, EBCL Outpatients) follow the same definition for selecting positive and negative pairs, where we censor some windows around the index event (EBCL Censored) or select different index event (EBCL Outpatients). On the contrary, OCP takes the swapped sequence (N, M) from the same patient to become the negative sample and the original ordered sequence (M, N) becomes the positive sample.
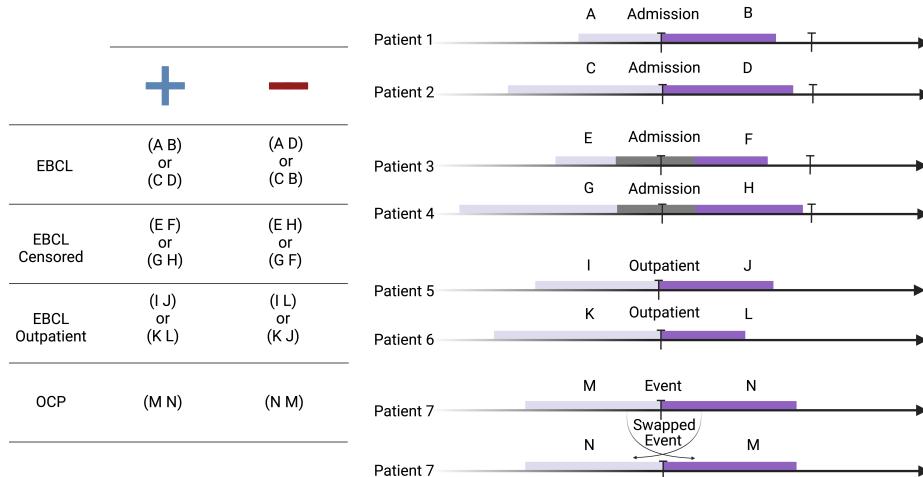

Figure 3: **Contrastive Learning Framework of EBCL, EBCL Ablations (EBCL Censored, EBCL Outpatient) and OCP.**

Due to this difference inherently arising from the definition of positive and negative samples, OCP (Agrawal et al., 2022) and EBCL have distinct potential for learning different types of features in a medical record. We can think of two different features that have x_1 a static nature that doesn't change frequently over time and x_2 a time-varying feature that changes over a short period of time. Under OCP pre-training, the value of feature x_1 is identical over two consecutive windows M and N. Thus, OCP pre-training cannot use the observed value of the feature to differentiate between a positive pair (M, N) and a negative pair (N, M) as both pairs agree on the feature value, so the model is not incentivized to capture the approximate value of the static feature in the produced embeddings at all.

Algorithm 1 Event-Based Contrastive Learning

Input: $(\text{pre}_i, \text{post}_i)_{i=1}^{N}$ pre, post time-series patient dataset pairs

for $epoch = 1$ **to** M **do**

    for $batch\_id = 1$ **to** K **do**

        Sample minibatch $(PRE, POST) = (\text{pre}_i, \text{post}_i)_{i=1}^{N/K}$;   `// encode pre and post`
        `trajectories`

        $PRE_f \leftarrow \text{transformer\_encoder}(PRE)$
        $POST_f \leftarrow \text{transformer\_encoder}(POST)$;   `// event based contrastive`
        `learning`

        $PRE_e \leftarrow \text{l2\_normalize}(\text{np.dot}(PRE_f, W_{pre}), \text{axis} = 1)$
        $POST_e \leftarrow \text{l2\_normalize}(\text{np.dot}(POST_f, W_{post}), \text{axis} = 1)$;   `// scaled pairwise`
        `cosine similarities`

        $\text{logits} \leftarrow \text{np.dot}(PRE_e, POST_e^T) \times \text{np.exp}(t)$;   `// symmetric loss function`
        $\text{labels} \leftarrow \text{np.arange}(n)$
        $\text{loss\_i} \leftarrow \text{CE}(\text{logits}, \text{labels}, \text{axis} = 0)$
        $\text{loss\_t} \leftarrow \text{CE}(\text{logits}, \text{labels}, \text{axis} = 1)$
        $\text{loss} \leftarrow (\text{loss\_i} + \text{loss\_t})/2$

    end

end

For EBCL, the value of the static feature agrees between positive samples, as it originates from the same patient. However, the value of the feature will disagree in the negative sample. Therefore, the EBCL model is incentivized to capture the approximate value of static features in its embeddings.

Let's now think about a feature that oscillates over time, which stays centered near a constant value, but oscillates with local temporal trends across both patients. Under OCP pretraining, the model can see that the trends observed in window M will directly continue into window N, which gives a strong signal that (M, N) is an appropriately ordered pair. In contrast, for a swapped sequence, the model will see that the trends do not continue from N to M, which clearly indicates an incorrectly ordered pair. Thus, this will be a strong signal for the model to differentiate positive (correctly ordered) from negative (incorrectly ordered) pairs, so the model will be incentivized to capture the local trends of oscillating features within windows M and N. Under EBCL pretraining, much like in OCP, the model can see that the trends observed in window A will directly continue into window B, which gives a strong signal that (A, B) is an appropriately ordered pair within the same patient. In contrast, for the negative pair (A, D) the model will be much less likely to observe a non-continuing pattern, which will be a clear negative signal. So, similar to OCP, the model is incentivized to capture the local trends of features within windows A and B in its embeddings. This is under the assumption that the feature is likely to be observed and retain its locally oscillatory behavior both near key events and distant from key events.
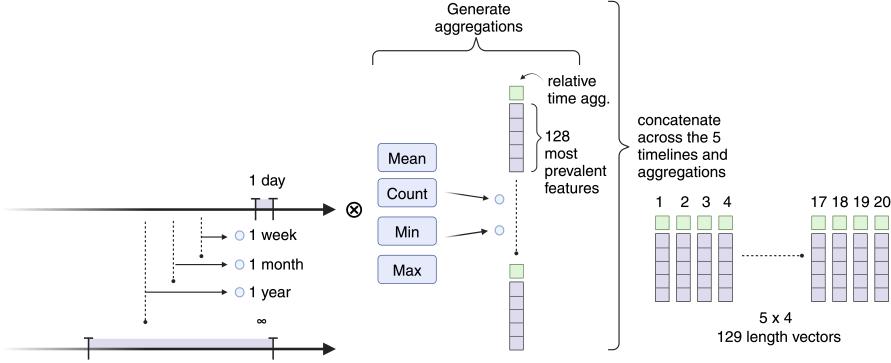
Figure 4: **XGBoost** requires a fixed size vector as input. We create this vector from time series data as follows: we restrict to the 128 most prevalent features in the data and the relative time of those observations (relative to the time of the decision). For each of the time windows prior to the time of the decision. For the heart failure cohort, windows end at discharge time for 1-Year Mortality and 30-Day Readmission and admission time for 7-Day LOS. For the MIMIC-IV cohort, windows end at the event time (i.e. hypotension or mechanical ventillation onset time). We perform feature aggregations (mean, count, min value, max value) for each feature over all pre-defined time windows. We then concatenate all of the feature aggregation outputs across all windows to get a final vector that is the input to XGBoost. We have 5 window sizes and 4 aggregations each generating a 129 length vector. After concatenating these, we get a 2,580 size vector that is the input for XGBoost.

Appendix B. Dataset and Experimental Setting

B.1. Dataset Preprocessing

We preprocess our heart failure dataset as follows: features with less than $1,000$ occurrences in the entire dataset are dropped. Categorical values with less than $1,000$ occurrences are replaced with the categorical value "UNKNOWN". We use the triplet embedding strategy from (Tipirneni and Reddy, 2022) for modeling sequential EHR data, and this allows flexibility in how dates are encoded. For all experiments, we encode dates as the relative time in days from the inpatient admission event divided by the standard deviation of these times in the training set. We label encode categorical observation values and features, and z normalize continuous data and feed it into a continuous value embedder to get a vector.

B.2. Task Definition

We pretrained the transformer on the time-series data around the domain knowledge-driven, cohort-specific important events for each patient. We have three pretrained models where each model was trained on one of three different cohort/event combinations: heart failure cohort on admission event, MIMIC-IV ICU cohort on hypotension event, and MIMIC-IV
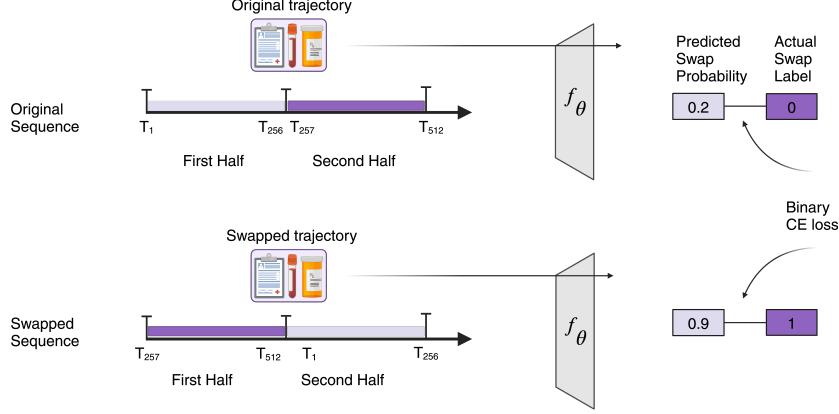
Figure 5: **OCP Positive and Negative Pairs**. In OCP, positive pairs are sequences with correct order, while negative pairs have the order of the first and second halves of the timeline swapped. The model, f_θ is pretrained to predict whether the sequence was swapped.
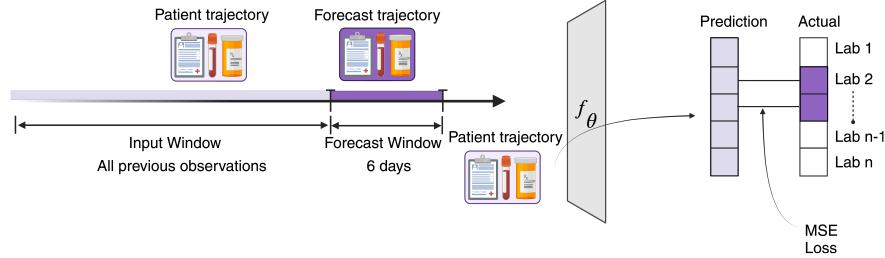

Figure 6: **STraTS** forecast patient trajectory in the forecasting window and is trained with Mean Squared Error (MSE) loss calculated on the observations present in the forecasting window.

ICU cohort on mechanical ventilation. Each model pretrained around the important event of each cohort is finetuned to predict the outcome for the same patient.

Table 8: Task Definition

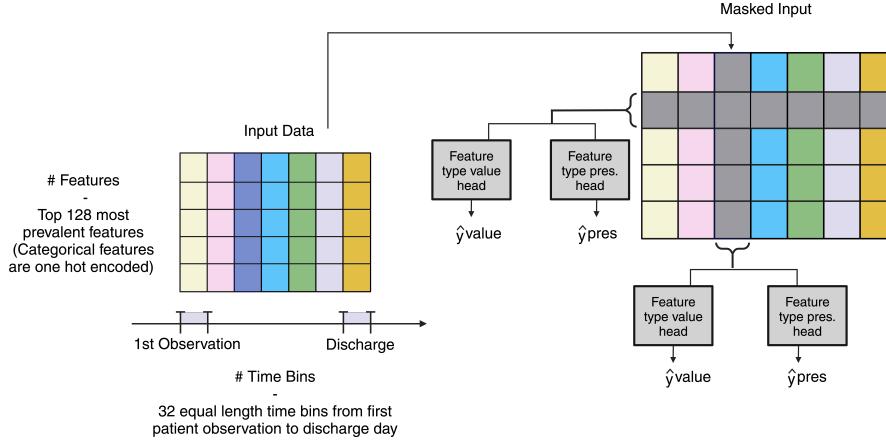| Dataset	Cohort/Event	Fine-tuning Task
Heart Failure	Inpatient Admission	Mortality/LOS/Readmission
MIMIC-IV	Hypotension	Mortality/LOS
MIMIC-IV	Mechanical Ventilation	Mortality/LOS

Figure 7: **DueTT** bins data into 32 time bins and a finite number of events as is depicted on the left side. For our admissions data this corresponds to binning data from the patient's first observation to their discharge time (or admission time for the LOS task). The pretraining task is to mask out a row (an event) and a column (a time bin) and predict the event values and event presences for the masked blocks.

B.3. Model Architecture and Training

Figure 8 summarizes the model architecture used for pretraining and finetuning for EBCL, OCP, STraTS, and fully supervised experiments.

Tokenization Method   We model patient trajectory data as a sequence of observations, represented as triples consisting of time (e.g., the time of observation), feature (e.g., a creatinine lab test), and value (e.g., the creatine lab test result) inspired by STraTS Tipirneni and Reddy (2022). We employ different encoders for each element of the triplet: a one-to-many feed-forward network for time, a one-to-many feed-forward network for continuous values, and a lookup table for embedding categorical features and values. These embeddings are then summed together to create the tokenized input for our model.

Hyperparameter tuning   For both our pretraining and finetuning, we perform the same hyperparameter search with 16 pairs of randomly sampled learning rates and dropouts. Learning rates are sampled from the log uniform distribution $(1e-6, 1e-2)$, and dropouts are sampled from the uniform distribution $(0, 0.6)$. We use the ASHA scheduler (Li et al., 2020) with a grace period of 4 epochs and a reduction factor of 2 to schedule the training of these jobs and select the trial with the best final validation loss. The ASHA scheduler will halt trials early in training that have a very high loss relative to other trials. Additionally, we use an early stopping tolerance of 3 epochs for all experiments except for OCP and DuETT which have more unstable training dynamics, in which case we use a tolerance of 10.
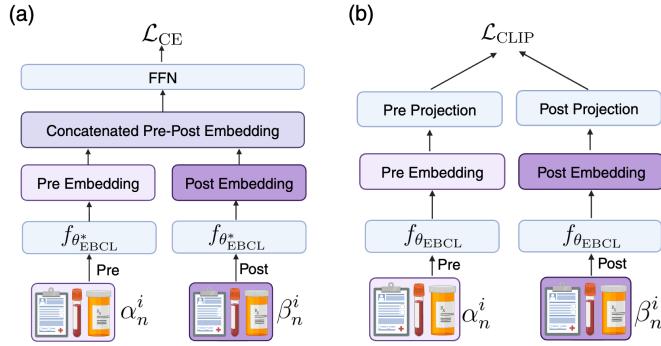
Figure 8: **Model Architectures**. FFN refers to a one hidden layer feed-forward network. **(a)** This architecture is used for EBCL, OCP, STraTS, and Supervised experiments. For EBCL we initialize θ with the final weights from EBCL pretraining, θ^*_{EBCL}, for OCP we initialize with the final weights from OCP pretraining, θ^*_{OCP}, and for Supervised we randomly initialize θ. Notice that Pre-event data and Post-event data are passed separately into the transformer encoder f_θ, so there is no self-attention between Pre-event and Post-event data. For Pre-event-only experiments, such as predicting 7-day LOS for the heart failure cohort, we leave out the 'Post Embedding' part of this architecture. **(b)** Architecture used for OCP Pretraining. The binary label for computing the cross-entropy loss, $\mathcal{L}_{\mathrm{CE}}$, is whether or not the random sequence, τ^i, is swapped. **(c)** Architecture used for EBCL Pretraining. The "Pre Projection" and "Post Projection" are linear projections, and their weights are not shared.

B.4. XGBoost

For the preparation of input dataset for XGBoost, we selected the 128 most prevalent features in our dataset and added the 129th feature for the relative time of these observations from admissions. We aggregate summary statistics (average, minimum, maximum, count) of the dataset within different windows (1 day, 1 week, 1 month, 1 year, ∞ years) from the decision date (Figure 4). For a fair comparison, we limit XGBoost to the same observations available in the EBCL pre and post windows (Table 3).

B.5. Order Contrastive Pretraining (Agrawal et al., 2022)

We prepare a continuous trajectory of 512 consecutive data points. This trajectory might either be maintained in its original order or have its two halves swapped (Figure 5. For the case where we keep the original ordering, the last data point, T_{256}, is set to time 0, with subsequent data points indicating the time elapsed since T_{256}. Alternatively, if we swap the trajectory, the last data point of the latter half, T_{512}, becomes time 0. Other data points then denote the time difference from T_{512}. We further adjust the dates of the initial half by adding the time gap, $T_{\text{GAP}} = T_{512} - T_{256}$. This adjustment ensures that the gap between T_{256} and T_{257} remains unaltered, regardless of whether the sequence is swapped or not.

For OCP pretraining we use the same transformer model as the EBCL experiments use, and for finetuning the same EBCL finetuning architecture displayed in figure 8 (a). Due to slow convergence, we allow up to a maximum of 300 epochs for pretraining. For fine-tuning, we load the OCP pretrained weights into our finetuning architecture in Figure 8.

B.6. STraTS (Tipirneni and Reddy, 2022)

STraTS represents time series as observation triplets, utilizing Continuous Value Embedding for time, feature, and values, and incorporates self-supervised learning for better generalization in data-limited scenarios. We implement the STraTS forecasting strategy for our dataset by randomly sampling a forecasting window with at least one observation in it and 16 observations prior to it. For the heart failure cohort, we use the median inpatient length of stay, 6 days, as our forecasting window length. For the MIMIC-IV ICU cohort, we use 2-hours just as STraTS did in their ICU experiments. All observations prior to the forecasting window (cutoff at a maximum of 512) are in our input window, and the STraTS pretraining task is to predict the data values in the prediction window. We calculate the Mean Squared Error (MSE) loss between features present in the forecast window with the forecasted output, as shown in Figure 6.

The input window is all data randomly sampled before the forecast window of 6 days, where we have at least 1 observation in the forecast window and 16 in the input window. All observations before the forecasting window (cutoff at a maximum of 512) are in our input window, and the pretraining task is to predict the data values in the prediction window, and the loss is computed over the subset of values that are observed in the prediction window (Figure 6). We use the same relative times as described for the original sequence in the OCP experiment. For STraTS pretraining we use the same transformer model as the EBCL experiments use, and for finetuning the same EBCL finetuning architecture (Figure 8 (a)).

B.7. DuETT (Labach et al., 2023)

We select the 128 most prevalent features in the dataset and bin the dataset into 32-time bins. We augment this two-dimensional matrix of input data with 128 features and 32-time bins by stacking the same size of the input matrix with the count of each feature within each time bin. We use two transformer encoder layers over the time dimension and two over the feature dimensions, as performed in the DuETT paper. See Appendix Figure 7 for a visual. We generally achieved the best performance pretraining on timebins covering pre and post-data combined, even when we finetuned on only pre or post-data, such as for the LOS task. For producing embeddings, we use a DuETT model pretrained on time bins covering pre and post-data. We generate a pre-embedding by inputting only pre event data and averaging the output tensor over the 128 feature dimensions and 32 time bin dimensions to get a single 24 dimensional pre data vector. We get a 24-dimensional post embedding the same way.

Appendix C. KNN

For our KNN Classifier experiments, we do a sweep over all combinations of the following parameters:

1. **Neighbor Weighting**: uniform or distance

2. **KNN Model**: Pre-and-Post or ensemble

3. **Distance Metrics** Cosine distance, Euclidean, or Euclidean with pre and post embeddings individually L2 normalized.

4. **Number of Neighbors** 10, 30, 100, 300, and 1000

Table 9: **K-Nearest Neighbors for Evaluating the Pretrained Embeddings.** We boldface the best performing model.

	30-Day Readmission		1-Year Mortality		1-Week LOS	
	AUC	APR	AUC	APR	AUC	APR
OCP	67.46 ± 0.36	84.00 ± 0.30	72.61 ± 0.39	84.68 ± 0.35	64.51 ± 0.29	61.90 ± 0.39
STraTS	60.49 ± 0.37	79.95 ± 0.34	64.06 ± 0.43	78.77 ± 0.41	57.84 ± 0.30	53.57 ± 0.41
DuETT	59.71 ± 0.38	79.32 ± 0.34	64.32 ± 0.42	78.06 ± 0.43	57.17 ± 0.30	53.16 ± 0.40
EBCL	$\mathbf{68.46 \pm 0.36}$	$\mathbf{84.89 \pm 0.28}$	$\mathbf{77.87 \pm 0.34}$	$\mathbf{88.21 \pm 0.28}$	$\mathbf{81.59 \pm 0.22}$	$\mathbf{81.66 \pm 0.25}$

For neighbor weighting, we either weigh the labels of neighbors uniformly or by the inverse of their distance. We detail KNN models in Figure 9. The tasks that use pre and post-representations (1-Year Mortality and 30-Day Readmission) use either of two KNN classifier models. For the `Pre and Post` KNN model, the pre and post-representations
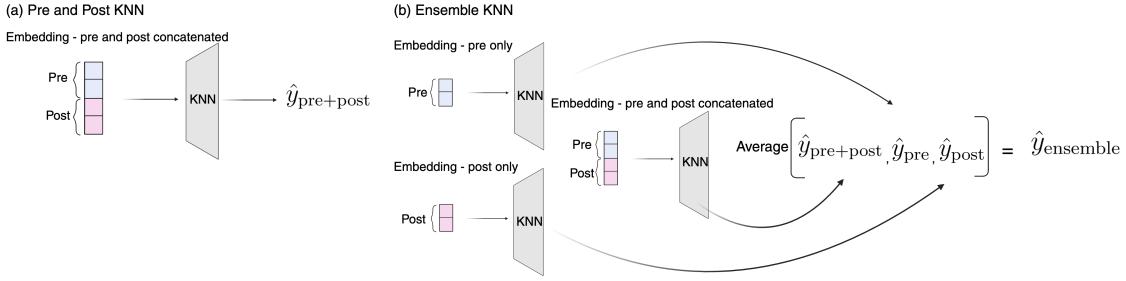
Figure 9: **KNN Models.** We try two KNN classifier strategies. The **Pre and Post** model concatenates the pre and post window representations before feeding them into the KNN. The **Ensemble** model averages the predicted class probabilities from three KNNs where: (1) $\hat{y}_{\text{pre}}$ = class probabilities from a KNN retrieving pre representation neighbors, (2) $\hat{y}_{\text{post}}$ = class probabilities from a KNN retrieving post representation neighbors, or (3) $\hat{y}_{\text{pre+post}}$ = class probabilities from a KNN retrieving neighbors of the concatenated pre and post representation.

are concatenated, and we fit a KNN classifier on these concatenated embeddings. For the `Ensemble` KNN model, we average the class probabilities from a `Pre and Post`, a pre-only, and a post-only KNN classifier. Note that for the 1-Week LOS task, we use only a pre-only KNN model. For each model's embeddings, we select the hyperparameter combination with the best validation set performance and report the test set performance of this configuration. To obtain standard deviations for K-NN results we use bootstrapping: we sample with replacement 1000 bootstraps from the testing dataset, and report mean and standard deviation of each metric computed with these samples. We achieve similar results to linear probing and again observe that EBCL significantly outperforms other baselines. Moreover, this analysis reveals that neighbors within the EBCL latent space are more similar in outcomes than those derived from any other baseline model, suggesting that EBCL inherently learns an outcome-related clustering structure through pretraining alone.

Appendix D. Results

We have analyzed the area under the precision-recall curve (AUPRC) across three different events and two datasets—HF dataset and MIMIC-IV ICU—applied to three distinct outcome prediction tasks. Consistent with the previously summarized AUROC results, EBCL outperformed other baseline methods when applied to the HF dataset (Table 10). It also excelled in three out of four event/task combinations for the MIMIC-IV ICU dataset (Table 12). Additionally, the linear probing results align with those observed in the AUROC assessments (Table 11, 13), demonstrating that the frozen weights of the EBCL model predict outcomes more accurately than the frozen embeddings from other baseline method-

ologies. This consistency reinforces EBCL's robustness and effectiveness in clinical outcome prediction across multiple settings.

Table 10: **EBCL Pretraining improves results over a supervised baseline and time-series pretraining baselines in the Heart Failure Dataset.** For the heart failure cohort, we summarize the downstream finetuning performance using both the area under precision recall curve (AUPRC) of three prediction tasks (30-Day Readmission, 1-Year Mortality, and 1-Week Length of Stay (LOS)) averaged over 5 runs with different seeds. We present finetuning performance on the MIMIC-IV Dataset for the outcomes of in-ICU Mortality and 3-Day LOS. Across all tasks, EBCL results (boldfaced) were statistically significantly better than all other tested models.

	Heart Failure Cohort		
	30-Day Readmission	1-Year Mortality	1-Week LOS
XGBoost	86.19 ± 0.03	89.58 ± 0.08	79.79 ± 0.08
S-Trans	85.60 ± 0.12	90.27 ± 0.15	88.61 ± 0.48
OCP	85.48 ± 0.20	89.36 ± 0.18	90.05 ± 0.28
STraTS	85.45 ± 0.07	89.31 ± 0.43	87.73 ± 2.03
DueTT	85.51 ± 0.31	89.04 ± 0.11	74.66 ± 0.62
EBCL	$\mathbf{86.40 \pm 0.03}$	$\mathbf{90.55 \pm 0.03}$	$\mathbf{90.96 \pm 0.04}$

Table 11: **Linear Probing for Evaluating the Pretrained Embeddings.** EBCL (boldfaced) yielded the embedding that performs the best across all tasks.

	30-Day Readmission	1-Year Mortality	1-Week LOS
OCP	82.50 ± 0.27	83.05 ± 0.56	55.08 ± 0.88
STraTS	79.94 ± 0.43	79.34 ± 0.89	53.34 ± 0.94
DuETT	78.44 ± 2.52	78.04 ± 4.82	50.32 ± 1.22
EBCL	$\mathbf{82.92 \pm 0.06}$	$\mathbf{85.85 \pm 0.23}$	$\mathbf{69.67 \pm 3.26}$

Appendix E. Ablations

E.1. Effect of Sampling Observations

The censoring window length was determined based on the EBCL window statistics analysis. Specifically, we selected the window to align with the 25th percentile for pre-event and post-event observations, according to the EBCL statistics. Excluding the 25th percentile of data

Table 12: **EBCL Pretraining improves downstream outcome prediction over a supervised baseline and time-series pretraining baselines in the MIMIC-IV cohort.** We summarize the finetuning performance using two metrics: area under the precision-recall curve (APR) of two prediction tasks (In-ICU Mortality and 3-Days Length of Stay (LOS)). The result has averaged over 5 runs with different seeds.

	MIMIC-IV Hypotension		MIMIC-IV Mechanical Ventilation	
	In-ICU Mortality	3-Day LOS	In-ICU Mortality	3-Day LOS
XGBoost	**55.34 ± 0.62**	55.64 ± 2.72	40.77 ± 0.78	40.29 ± 0.41
S-Trans	44.01 ± 0.72	76.97 ± 0.26	45.97 ± 15.44	79.62 ± 0.49
OCP	43.27 ± 0.44	76.76 ± 0.26	55.78 ± 0.49	79.49 ± 0.29
STraTS	44.65 ± 0.45	76.69 ± 0.09	55.78 ± 0.49	79.49 ± 0.29
DueTT	31.43 ± 1.32	71.79 ± 1.24	14.89 ± 0.50	54.63 ± 9.00
EBCL	46.02 ± 0.10	**77.23 ± 0.06**	**55.98 ± 0.72**	**80.96 ± 0.11**

Table 13: **Linear Probing for Evaluating the Pretrained Embeddings.** EBCL (bold-faced) yielded the embedding that performs the best across all tasks.

	MIMIC-IV Hypotension		MIMIC-IV Mechanical Ventilation	
	In-ICU Mortality	3-Day LOS	In-ICU Mortality	3-Day LOS
OCP	31.61 ± 1.46	68.62 ± 0.93	21.60 ± 2.12	65.12 ± 0.68
STraTS	32.73 ± 2.03	69.19 ± 1.20	27.96 ± 1.80	67.02 ± 0.90
DueTT	31.14 ± 1.41	72.16 ± 0.58	15.13 ± 0.04	63.73 ± 0.27
EBCL	**38.35 ± 0.94**	**73.94 ± 0.44**	**35.00 ± 2.07**	**73.89 ± 1.03**

preceding and following the event onset led to the exclusion of 260 observations pre-event and 60 observations post-event.

Appendix F. Risk Stratification and Patient Subtyping with EBCL

F.1. Deep Clustering of EBCL Embedding

From the EBCL pretrained transformer, we build pre-event and post-event vector representations for each admission in the test set to form a concatenated transformer embedding that includes comprehensive information pre- and post-event. For clustering our representations, we use K-means clustering and find the optimal K using the elbow method. This entails plotting within-cluster similarity vs the number of clusters and using an elbow de-

Table 14: **Ablation Studies**. We compare the EBCL variants by applying various definitions of events and different sampling strategies. We summarize the downstream finetuning performance (AUPRC) of three prediction tasks averaged over 5 runs with different seeds, where we boldface statistically significant results. *Note that FT stands for finetuning data and the entry both means both pre and post data are used, but for predicting 1-Week LOS we always only used the Pre-event dataset to avoid data leakage.

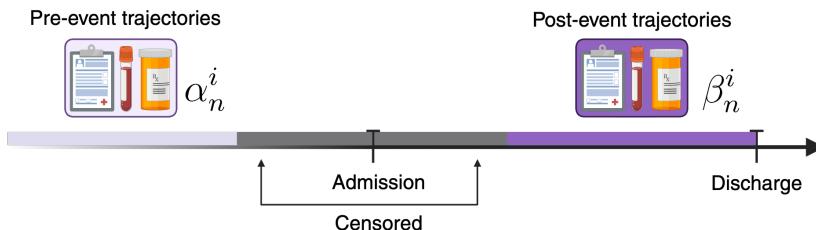|	Index Event	FT*	30-Day Readmission	1-Year Mortality	1-Week LOS
EBCL	Inpatient	Both	**86.40 $\pm$ 0.03**	**90.55 $\pm$ 0.03**	**90.96 $\pm$ 0.04**
Censoring	Inpatient	Both	85.83 $\pm$ 0.04	90.08 $\pm$ 0.02	90.35 $\pm$ 0.12
Non-Adm	Non-Inpatient	Both	85.75 $\pm$ 0.05	90.45 $\pm$ 0.06	90.06 $\pm$ 0.18
Outpatient	Outpatient	Both	85.66 $\pm$ 0.11	90.34 $\pm$ 0.02	89.64 $\pm$ 0.12
Pre Event	Inpatient	Pre	85.70 $\pm$ 0.06	88.89 $\pm$ 0.05	✗
Post Event	Inpatient	Post	85.11 $\pm$ 0.06	89.41 $\pm$ 0.01	✗

Figure 10: **EBCL - Censoring Ablation**. We censor a fixed number of observations from the end of the pre window and beginning of the post window and take the 512 remaining closest observations before the admission as pre data and after the admission and post data.

tection method (Satopaa et al., 2011) to find the point of maximum curvature which is the optimal $K = 6$ for EBCL embeddings.

We use dimensional reduction with Uniform Manifold Approximation and Projection (UMAP) (McInnes et al., 2018) for the ease of visualization of our high-dimensional data. The identified clusters that were found are superimposed over the resulting UMAP graphic to highlight the separation and distribution of the clusters in the reduced-dimensional space in Figure 11 (a). To understand the phenotype of each cluster, we compare the outcome of patients in each identified cluster (years to mortality, days to readmission, the prevalence of 1-year mortality, and 30-day readmission) (Figure 11). To further validate the prognos-

Table 15: **Results for finetuning only using pre-admission (Pre-event) data.**

	30-Day Readmission		1-Year Mortality	
	AUC	APR	AUC	APR
XGBoost	69.86 ± 0.03	85.35 ± 0.02	77.27 ± 0.04	87.76 ± 0.02
Supervised	68.27 ± 0.16	84.37 ± 0.15	77.36 ± 0.19	87.42 ± 0.20
OCP	68.83 ± 0.13	84.63 ± 0.08	77.93 ± 0.13	87.85 ± 0.04
STraTS	68.46 ± 0.04	84.34 ± 0.18	78.18 ± 0.63	87.89 ± 0.52
DueTT	68.23 ± 0.11	84.97 ± 0.03	75.14 ± 0.37	86.17 ± 0.23
EBCL	70.48 ± 0.09	85.70 ± 0.06	79.63 ± 0.06	88.89 ± 0.05

Table 16: **Results for finetuning only using post-admission (Post-event) data.**

	30-Day Readmission		1-Year Mortality	
	AUC	APR	AUC	APR
XGBoost	68.05 ± 0.10	84.80 ± 0.04	77.12 ± 0.17	87.54 ± 0.16
Supervised	68.68 ± 0.08	84.69 ± 0.05	79.77 ± 0.21	88.92 ± 0.19
OCP	68.49 ± 0.10	84.59 ± 0.05	79.23 ± 0.13	88.58 ± 0.07
STraTS	67.61 ± 0.16	84.05 ± 0.10	79.60 ± 0.12	88.71 ± 0.10
DueTT	67.47 ± 0.09	84.14 ± 0.06	76.47 ± 0.74	87.15 ± 0.35
EBCL	69.20 ± 0.09	85.11 ± 0.06	80.36 ± 0.03	89.41 ± 0.01

Table 17: **Comparative Analysis of One-Year Mortality and 30-Day Readmission Rates Across Patient Clusters Derived from Different Embedding Strategies.** Note that the one-year mortality prevalence in the test data is 31.09%. The 30-Day readmission prevalence is 26.66%.

	1-Year Mortality (%)			30 Days Readmission (%)		
Cluster	Cluster 1	Cluster 2	Δ prevalence	Cluster 1	Cluster 2	Δ prevalence
OCP	23.46	33.18	9.72	19.86	28.43	8.57
STraTS	30.96	31.64	0.68	26.25	28.75	2.50
DueTT	28.07	34.16	6.09	25.09	27.96	2.87
EBCL	28.00	50.87	22.87	23.52	34.53	11.01

tic differentiation between the identified heart failure subgroups, we plotted Kaplan-Meier (KM) (Dudley et al., 2016) survival curves of the patients in each cluster in figure 11 (b). This approach allowed us to visually and statistically compare the distribution of time-to-event of patients in the clusters.

F.2. Risk Stratification

We initialized the model with the pretrained model weights of all baseline models (EBCL, OCP (Agrawal et al., 2022), STraTS (Tipirneni and Reddy, 2022), DuETT (Labach et al., 2023)) and concatenated the pre- and post-event embeddings of the test set patients. We applied UMAP (McInnes et al., 2018) to reduce the dimensionality of the embeddings and to easily visualize our high dimensional data. Furthermore, we applied K-means clustering with $k = 2$ on the pretrained embeddings to subgroup the patient cohort by outcome risk. Using the identified clusters, we evaluated the survival outcomes with the Kaplan-Meier estimator (Dudley et al., 2016), which provided a visual representation of the survival probability over time for each cluster. To quantitatively compare the prognosis of two identified clusters (Cluster 1 and 2), we compare days to mortality and days to readmission between Cluster 1 and Cluster 2 (Figure 11, Table 17).
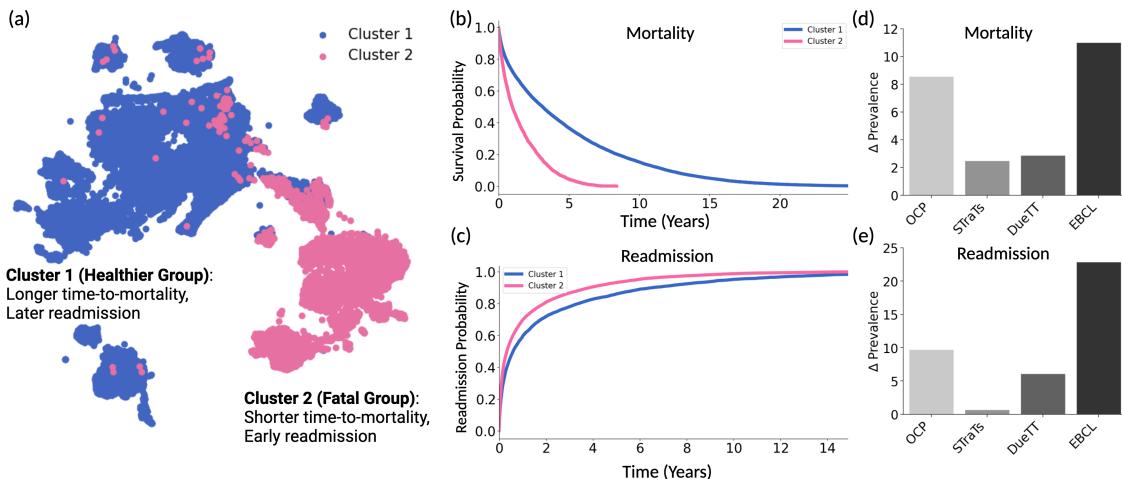

Figure 11: **Clustering and outcome risk subtyping from pretrained EBCL Embedding. (a)** Clustering and dimensionality reduction of pretrained embedding showed distinct heart failure clusters with unique outcome prognoses. Clusters are sorted by prevalence of 1-Year Mortality in each, thus cluster 1 has the highest 1-Year Mortality and represents the sickest group, and cluster 6 represents the healthiest. **(b)** Mortality survival curve of the same clusters from Figure (a). **(c)** Plot of the proportion of population readmitted over time for the same clusters from Figure (a).

Our analysis revealed statistically significant disparities in outcome prevalence among the clusters identified by various predictive models, including EBCL, OCP (Agrawal et al., 2022), and STraTS (Tipirneni and Reddy, 2022). Specifically, using a two-sampled Student's t-test, we found that Cluster 2 in the EBCL model demonstrated a statistically significant higher one-year mortality rate at 50.87 compared to 28.00 in Cluster 1 (Table 17). This trend was consistent across other models, with the EBCL model showing the highest gaps in prevalence, reinforcing its robustness in stratifying patient risk. However, the clusters

identified with STraTS (Tipirneni and Reddy, 2022) on the 1-Year Mortality task didn't show patient subgroups that are with statistically significantly different prognoses.

Notably, the EBCL model showed better stratification of patients, evidenced by high gaps of prevalence between clusters compared to other baselines (22.87 for one-year mortality and 11.01 for 30-day readmission tasks, respectively. (Table 17, Δ prevalence column), Figure 11 (d), (e)). These insights demonstrate the capacity of EBCL to generate clinically meaningful representations, potentially aiding in more effective patient stratification and personalized healthcare based on patient phenotyping.